Crimson Publishers
Wings to the Research

Short Communication

Synthesis and Characterization of Nickel Doped Iron Oxide Nano Particles for Biomedical Application

Arshad Javid Muhammad* and Abbas Adeel

Department of Basic Sciences, University of Engineering & Technology, Pakistan

ISSN: 2694-4391

***Corresponding author:** Muhammad Arshad Javid, Department of Basic Sciences, University of Engineering & Technology, Pakistan

Submission: October 10, 2021

Published: November 23, 2021

Volume 2 - Issue 5

How to cite this article: Arshad Javid Muhammad, Abbas Adeel. Synthesis and Characterization of Nickel Doped Iron Oxide Nano Particles for Biomedical Application. Int J Conf Proc. 2(5). ICP. 000549. 2021.
DOI: 10.31031/ICP.2021.02.000549

Abstract

The objective of this work is to synthesize and characterization of nickel ferrite as MRI contrast agent to improve the signal intensity of T2 weighted images for biomedical application. For structural analysis, XRD was revealed that Ni-doped Fe_2O_4 have a cubic spinal structure Having Miller Indices (hkl) values of (220), (311), (222), (400), (331), (442), (333), (440) and (531). From XRD data, the grain size of Ni Fe2O4 was observed to be (17.12nm) after 20wt.% Ni-doped Fe_2O_4, and its further increases up to19.36nm for 40wt.% Ni Fe_2O_4, respectively. The XRD pattern confirmed that doping of Ni metal increased the grain size of nanoparticles. SEM was performed to study the morphology of prepared samples. EDX was performed to confirm the elemental analysis. EDX spectra depicted the desired peaks of Fe, O, Cl, and Ni for Ni-doped Fe_3O_4. Saturation magnetization (Ms) was improved with concentration of dopant material Ni (20wt.%, 40wt.%) in magnetic nanoparticles. In essence, this study demonstrates the very easy way of synthesis of Ni doped iron oxides nanoparticles for biomedical applications as MRI contrast agents

Keywords: Nickel ferrites; Magnetic nanoparticles; MRI contrast agents; T2-Weighted

Introduction

Magnetic nanoparticles were significantly studied for biomedical research such as drug delivery, hyperthermia in cancer, protein separation, biosensing and Magnetic Resonance Imaging (MRI) [1-3]. Since the late 1990s, iron oxide-based nanoparticle contrast agents have been explored and clinically used as T2-weighted contrasts agents. They compose magnetic nanoparticle core and biocompatible coating material, preventing aggregation and sedimentation and allowing high biological tolerance [4]. Recently, researchers have focused on nickel ferrite nanoparticles as MRI contrast agents due to their high magnetic susceptibility, biocompatibility, biodegradability and nontoxicity characteristics [5]. Several studies have investigated the nickel-based nanoparticles as an alternative to gadolinium for reducing the risk of toxicity [6]. Nickel metal also possesses a high spin quantum number and proton exchange kinetics [7]. MRI has several blessings over unique imaging modalities due to excessive spatial selection, amazing clean tissue evaluation and non-utilization of radioisotopes. Paramagnetic gadolinium complexes are commonly used as MRI contrast agent [8]. However, gadolinium-based complexes have low sensitivity and have toxic outcomes that incorporate Nephrogenic Systemic Fibrosis (NSF) [9]. Moreover, most gadolinium complexes are designed to circulate time, precluding excessive decisions and focusing on MRI quickly. The signal intensity is a function of T2 relaxation, i.e., $I \sim M_o\, e^{-t/T2}$ was used to determine the T2 relaxation times. In this research work, nickel dopped iron oxide nanoparticle have been synthesized using co-precipitation method to enhance its sensitivity as T2-W contrast agents.

Experimental

Ferric chloride hexahydrate ($FeCl_3.H_2O$), ferrous chloride tetrahydrate ($FeCl_2.H_2O$), nickel chloride hexahydrate ($NiCl_2.H_2O$) and ammonium hydroxide (NH_4OH) were used for the preparation of Fe_3O_4 and $NiFe_2O_4$ superparamagnetic nanoparticles using co-precipitation method. Distilled water was used as a solvent to remove the impurities in the final product. Oleic acid was used as a surfactant [3]. First, the solution of $NiCl_2.6H_2O$ was prepared in distilled water and stirrered for 1 hour at at 50 °C approximately. Then the solution of $FeCl_2.4H_2O$ was prepared in the distilled water and stirrered for 1 hour at 50 °C. Then solutions of $NiCl_2.6H_2O$ and $FeCl_2.4H_2O$ were mixed with continuous stirring at 70 °C. Then NaOH was added drop wise upto pH 12. Oleic acids were added in the same solution as a capping agent and surfactant. The precipitation was washed out with distilled water and dried in the oven at 80 °C for 6 hours. The synthesized nickel ferrites were grinded into a fine powder. The chemical reaction of the $NiFe_2O_4$ has been mentioned as in equation-1.

$$2Fe^{3+} + Ni^{2+} + 8OH^{-1} \rightarrow NiFe_2O_4 + 4H_20 \quad (1)$$

Results and Discussion

X-Rays Powder Diffraction (XRPD)

Nidoped ferrites was analyzed with X-ray diffractometer using Cu as a targeted source of X-rays production with Kα_1 radiation having the wavelength of λ=1.54 Å. The powder sample was evaluated in the angle range of 2θ=10110° at the scanning speed of 0.02°/min and step size of 0.031° and step time of 0.3 sec. Powder samples of undoped and Ni-doped ferrites showed crystalline nature as shown in Figure 1. XRD pattern for Ni-doped iron oxide $Ni_{0.2}\,Fe_{2.8}\,O_4$ and $Ni_{0.4}\,Fe_{2.6}\,O_4$. was shown in Figure 1. Diffracting peaks of all prepared samples were depicted in Figure 1 at 2θ = 29.94°,35.57°,37.13°,43.32°,47.33°,54.11°,57.21° and 62.95° with miller indices (220), (311), (222), (400), (331), (422), (333) and (440) respectively (Table 1).

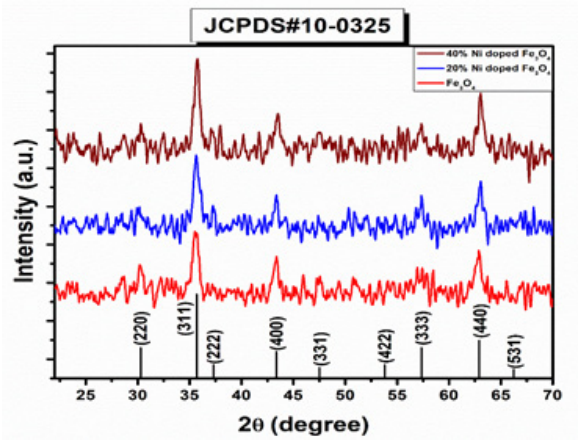

Figure 1: XRD pattern of $NiFe_2O_4$.

Table 1: XRD analysis of the $NiFe_2O_4$.

Composition	2θ (deg)	FWHM (deg)	hkl	Crystalline Size (nm)	a (Å)
$Ni_{0.2}\,Fe_{2.8}\,O_4$	35.62	0.6287	(311)	13.26	8.34
$Ni_{0.4}\,Fe_{2.6}\,O_4$	35.75	0.5904	(311)	14.13	8.32

The XRD diffraction peaks of the $Ni_{0.2}\,Fe_{2.8}\,O_4$ (S_2), and $Ni_{0.4}\,Fe_{2.6}\,O_4$ (S_3), belongs to the FCC structure, which can be well-matched with (JCPDS) card no (000100325). Diffraction peaks and their sharpness define the degree of crystallinity. There are no other extra secondary phases, suggesting that the ions of Ni^{2+} are entirely diffused into the Asite which is Fe^{2+} in Fe_3O_4. For the calculation of the lattice parameter following relation was used:

$$a = d_{hkl}(\sqrt{h^2 + k^2 + l^2} \quad (2)$$

$$n\lambda = 2d\sin\theta \quad (3)$$

For the calculation of crystallite size following equation was used:

$$D = \frac{KX\lambda}{\beta \times \cos\theta} \quad (4)$$

Where D represents the crystallite size of the diffraction peak, K represents the shape factor of the particles which is 0.9, λ is the wavelength of the radiation has the value 1.54 Å,β is the full width at half maxima of the diffraction peak, and θ is the corresponding Bragg's diffraction angle Table 2.

Table 2: Average grain size $NiFe_2O_4$.

Sr. No	Material	Grain Size (nm)
2	Ni-Fe_3O_4(20%wt)	17.12
3	Ni-Fe_3O_4(40%wt)	19.36

SEM analysis

The surface morphology of Nidoped Fe_3O_4 was studied through SEM model Instrument JSM5910, Japan at 20.0kV. SEM confirmed that particles are spherical in shape and most of them are in flask shape [10]. The density of the particles was also increased with the increase in the concentration of Ni in Fe (Figure 2).

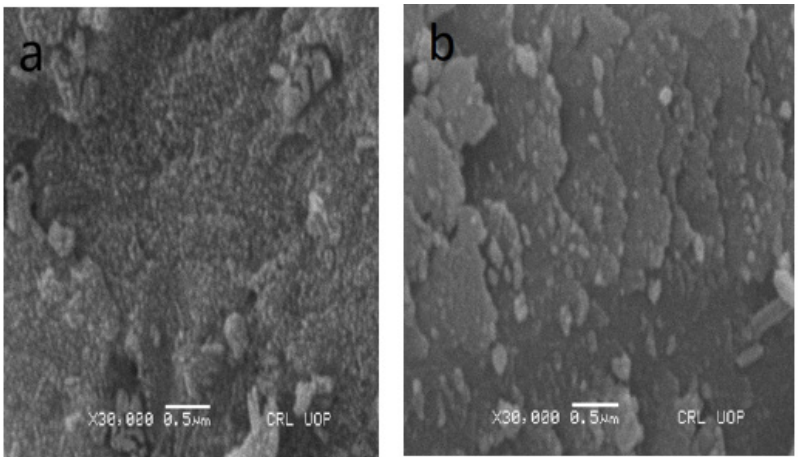

Figure 2: SEM images of undoped and Ni-doped Fe3O4
a. 20% Ni-doped Fe_3O_4 and
b. 40% Ni-doped Fe_2O_4.

Vibrating Sample Magnetometer (VSM)

Magnetic properties of prepared samples such as saturation magnetization were measured at room temperature using Dexing Magnet Tech Co, Model (VSM100), China. Nidoped Fe_2O_4 nanoparticles did not depicted hysteresis curve. This saturation magnetization confirmed that all the samples have superparamagnetic behavior in nature. The magnetization curve showed high saturation magnetization and low coercive force. The saturation magnetization was increased from 48.96emu/cm^3 to 126.7emu/cm^3. When high concentration of Ni^{2+} shifts the Fe^{3+} ions from tetrahedral site to the octahedral site, then the tetrahedral site-to-octahedral site interactions increases, and the octahedral-to-octahedral interactions decreases. The total magnetic moment of the system is increased and therefore the magnetization of the system also increases. It was observed that the coercivity of the system decreases with the increasing content of Ni substitution. When the 20wt.% and 40wt.% nickel is incorporated in ferrite the maximum saturation magnetization was increased up to 115.55emu/cm^3 and 126.7emu/cm^3 respectively also the remanence was increased to 19.92emu/cm^3 and then decrease to 19.50emu/cm^3 for 20% Ni dope Ni and 40% Ni doped ferrite, respectively. There is no detectable change observed in coercive field values that are 0.0094 and 0.0095 T for 20% Ni-doped Ni and 40% Ni-doped ferrite, respectively. The Maximum saturation magnetization (M_s), Remanence (M_r), the ration of M_r/M_s, and coercive field values for undoped and Ni doped ferrites was listed in Table 3.

Table 3: Magnetic properties of Ni ferrites.

Samples	Saturation Magnetization (M_s) emu/cm_3	Remanence (M_r) emu/cr_3	M_r/M_s	Coercivity Field (H_c) (T)	Magnetic Moment (μβ)
Ni-Fe_3O_4(20%wt)	115.55	19.92	0.172	0.0094	4.84
Ni-Fe_3O_4(40%wt)	126.7	19.5	0.153	0.0095	5.31

Where H_c represents the coercive field and M_s shows saturation magnetization, while anisotropy constant value K depends upon the concentration of dopant material. It means that the anisotropy constant of the system increases with the increasing content of Ni (Figure 3).

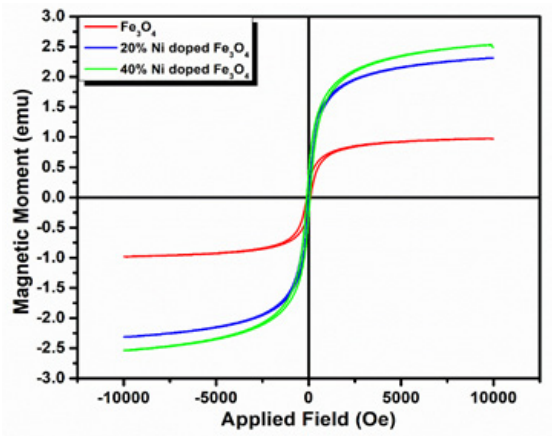

Figure 3: M-H loop for undoped and Ni-doped Fe_3O_4.

Conclusion

In this study, Nidoped iron oxides nanoparticles were prepared using co-precipitation method at room temperature. The structural conformation was done with XRD which exhibit spinal cubic structure of magnetic nanoparticles. From XRD data, the average grain size of Ni Fe_2O_4 from 17.12nm to 19.36nm after doping of Ni with 20wt.% and 40wt.%, respectively. The surface morphology of samples revealed that particles depicted the flat surface and have negligible agglomeration in SEM analysis. The saturation magnetization for $NiFe_2O_4$ was enhanced 115.55, to 126.7emu/cm^3 after Ni doping with 20wt.% and 40wt.% Ni, respectively. Therefore, this study concludes that nickel ferrites may be used in diagnostic modality to see the pathology of the organ as T2-W contrast agents for biomedical applications.

References

1. Bai C, Hu P, Liu N, Feng G, Liu D, et al. (2020) Synthesis of ultrasmall Fe_3O_4 nanoparticles as T_1-T_2 dual-modal magnetic resonance imaging contrast agents in rabbit hepatic tumors. ACS Applied Nano Materials 3(4): 3585-3595.
2. Vangijzegem T, Stanicki D, Panepinto A, Socoliuc V, Vekas L, et al. (2020) Influence of experimental parameters of a continuous flow process on the properties of Very Small Iron Oxide Nanoparticles (VSION) designed for T_1-weighted Magnetic Resonance Imaging (MRI). Nanomaterials 10(4): 757.
3. Thomsen HS (2014) Nephrogenic systemic fibrosis and gadolinium-based contrast media. Springer, pp: 207-217.
4. Senpan A, Caruthers SD, Rhee I, Mauro NA, Pan D, et al. (2009) Conquering the dark side: Colloidal iron oxide nanoparticles. Acs Nano 3(12): 3917-3926.
5. Vuong QL, Berret JF, Fresnais J, Gossuin Y, Sandre O, et al. (2012) A universal scaling law to predict the efficiency of magnetic nanoparticles as MRI T($_2$)-contrast agents. Adv Healthc Mater 1(4): 502-512.
6. Ward KM, Aletras AH, Balaban RS (2000) A new class of contrast agents for MRI based on proton Chemical Exchange Dependent Saturation Transfer (CEST). Journal of magnetic resonance 143(1): 79-87.
7. Dula AN, Smith SA, Gore JC (2013) Application of Chemical Exchange Saturation Transfer (CEST) MRI for endogenous contrast at 7 Tesla. Journal of Neuroimaging 23(4): 526-532.
8. Mao Z, He Y, Zhao H, Zhang Y, Yin J, et al. (2020) A positively charged small-molecule T_1 magnetic resonance imaging contrast agent for highly efficient labeling and tracking adipose tissue-derived stem cells. Materials Today Communications 25: 101627.
9. Maheshwaran D, Nagendraraj T, Balaji TS, Kumaresan G, Kumaran SS, et al. (2020) Smart dual T_1 MRI-optical imaging agent based on a rhodamine appended Fe(III)-catecholate complex. Dalton Transactions 49(41): 14680-14689.
10. Hu P, Kang L, Chang T, Yang F, Wang H, et al. (2017) High saturation magnetization Fe_3O_4 nanoparticles prepared by one-step reduction method in autoclave. Journal of Alloys and Compounds 728: 88-92.